URN (Paper): urn:nbn:de:gbv:ilm1-2011iwk-111:3

56TH INTERNATIONAL SCIENTIFIC COLLOQUIUM
Ilmenau University of Technology, 12 – 16 September 2011
URN: urn:nbn:gbv:ilm1-2011iwk:5

# LARGE-SCALE TEST RIG FOR ASSESSMENT OF CHARACTERISTICS OF FLAT AIR BEARINGS RUNNING AGAINST A ROTATING COUNTER-FACE

*Calonius, O.; Kiviluoma, P.; Kuosmanen, P.*

Aalto University School of Engineering, Department of Engineering Design and Production,
P.O. Box 14100, FI-00076 AALTO, Email: olof.calonius@aalto.fi

## ABSTRACT

Air bearing technology could provide a competitive "green" alternative to conventional bearings if high enough load carrying capacity as well as tolerance for low surface quality could be obtained and combined with the naturally low friction of the air bearings. There are numerous benefits of the reduced friction, for example, in machinery smaller drives can be used and thermal stability of components is improved. Naturally these benefits must be weighed against the energy consumption of compressors used for producing air for the bearings. Therefore, air flow through the bearings should be kept at a reasonable level.

In this paper, a test rig for studying the operating characteristics of air bearings is presented. In the test rig it is possible to run thrust bearings against a relatively large rotating circular counter surface. Two types of bearing units have been studied: a traditional, orifice compensated air bearing and a porous material air bearing. Results on bearing characteristics such as load carrying capacity and stiffness are reported as well as the influence of axial run-out on load and air gap height during rotation of the counter surface.

***Index Terms*** – Porous air bearings, orifice compensated, experimental, synchronized averaging

## 1. INTRODUCTION

Air bearings are typically used in applications where frictionless and precise motion is needed, such as, in coordinate measuring machines. In precision machining air bearing spindles allow very high speeds. There are also air bearing applications in the robust industrial systems for moving heavy loads on factory floor, such as in the production of huge electrical transformers or diesel engine blocks. While the majority of industrial applications still rely on roller bearing or oil lubricated sliding bearing technology, there is an increasing demand for reduced power consumption. In some cases, air bearing technology could provide a competitive "green" alternative to conventional bearings if we could obtain high load carrying capacity and tolerance for low surface quality combined with the naturally low friction of the air bearings. There are numerous benefits of the reduced friction, for example, smaller drives can be used and thermal stability of components is improved. Naturally these benefits must be weighed against the energy consumption of compressors used for producing air for the bearings. Therefore, air flow through the bearings should be kept at a reasonable level.

Aerostatic bearings are typically characterized by load capacity, stiffness and air consumption. To find out these characteristics, it is necessary to measure bearing load, air gap height and air flow. Measurements are usually done with special equipment in laboratory conditions. Typically the equipment is based on a solid, rigid counter surface, such as granite table, and the load is applied in a vertical direction. This kind of setup has the benefit of using gravity as a loading element so that the load can be adjusted, for example, by adding weights [1], [2]. Other ways used to provide load are pneumatic cylinders [3], [4] and screws [5]. Dynamic load variations can be achieved using electromagnetic [3], [6] or piezoelectric shakers. The height of the air gap is usually measured using three symmetrically positioned displacement sensors, such as, capacitive, inductive or eddy current sensors [1], [3], [6]. This configuration makes it possible to detect the alignment of the bearing as well.

In this paper, a test rig for studying the operating characteristics of thrust air bearings is presented. In typical applications for aerostatic bearings the relative transversal velocity between the bearing and counter surface is low, but in the test rig presented here it is possible to have thrust bearings running against a relatively fast moving circular counter surface and it is possible to study new concepts for air bearings for conditions where they have not yet been utilized.

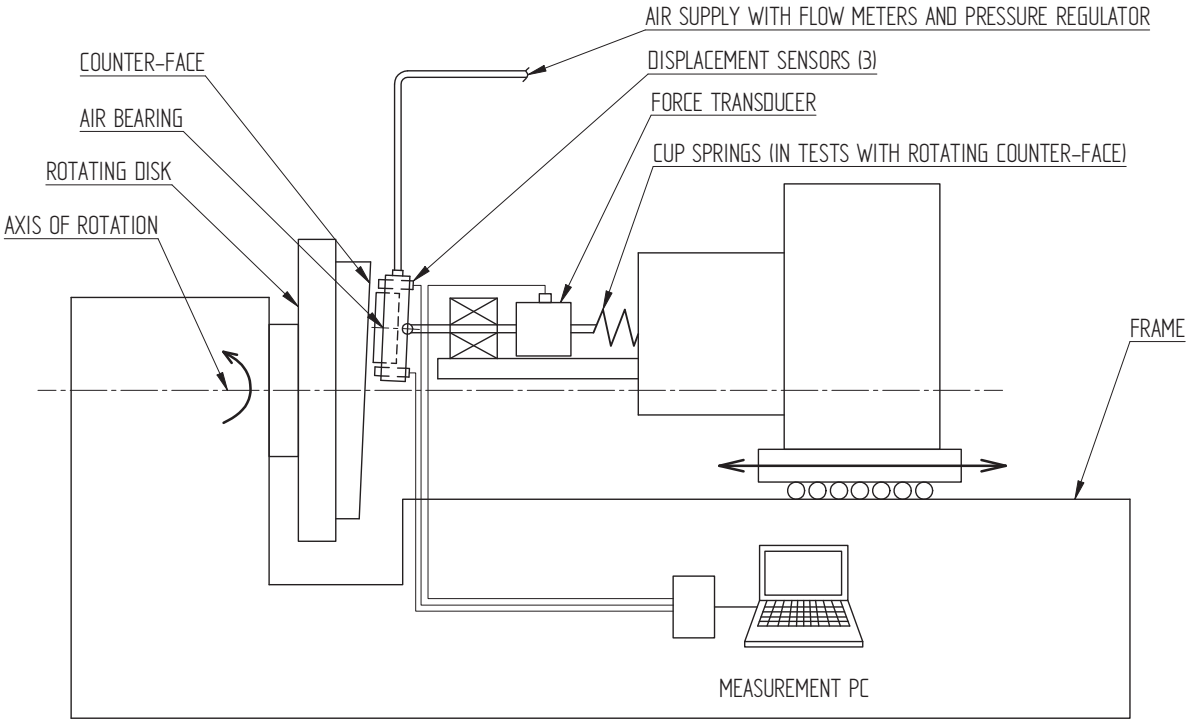


**Figure 1. Schematic of the test rig.**

To find out the performance and properties of the test rig, two types of bearing units were studied: a traditional, orifice compensated air bearing and a porous type air bearing. In applications involving large bearing surfaces, the challenge is to maintain reasonable energy efficiency by minimizing air leakage, especially in conditions where run-out and variations in surface quality of the counter surface exist. There may also be significant fluctuations in the load. The tests will provide information on how the operating parameters, such as, input pressure, preload and gap height affect the bearing behavior.

## 2. METHODS

The test rig is used to study the characteristics of flat pad aerostatic bearings. The main requirements in constructing the test rig were as follows. Measurements should include static load versus air gap height measurements (with a non-rotating counter-face) for determining the stiffness of the bearing. At the same time, air consumption should be monitored. Because axial run-out and changes in operating conditions can cause collisions between the bearing and the counter-face, measurements should be possible also when the counter-face is rotating. These dynamic measurements should involve studying the effect of changes in sliding speed, loading, axial run-out and supply pressure on the air gap height. The load should be adjustable from zero up to a few thousand newtons. The air gap measurement should be done in a micro meter range.

### 2.1. Test rig structure

A large-size lathe (1M65) was chosen as a basis for the test rig because of the rigid structure and precise guide ways. It also offers a simple mechanism to adjust both the relative movement between the bearing and counter surfaces and the air gap height. The speed of rotation of the counter face can be controlled in a range from 5 rpm to 500 rpm. The maximum diameter of the counter-face, limited by the chuck, is 1000 mm. The axial run-out can be adjusted by misaligning the counter-face relative to the axis of rotation. The principle of the test rig is shown in Figure 1.

### 2.2. Loading and load measurement

The loading force is adjusted by hand screw of the tool slide in the lathe. A force transducer, attached to the bearing support, measures the bearing load. The test bearing is mounted to the end of a shaft by a threaded stud and a ball joint. The ball joint ensures the parallelism between the surfaces. The 20 mm diameter shaft is guided by aerostatic bearings (New Way S302001) which allow frictionless axial movement. The force transducer (HBM U2B 5 kN) is mounted in series with the shaft by a threaded joint. The end of the force sensor rests against a fixed end.

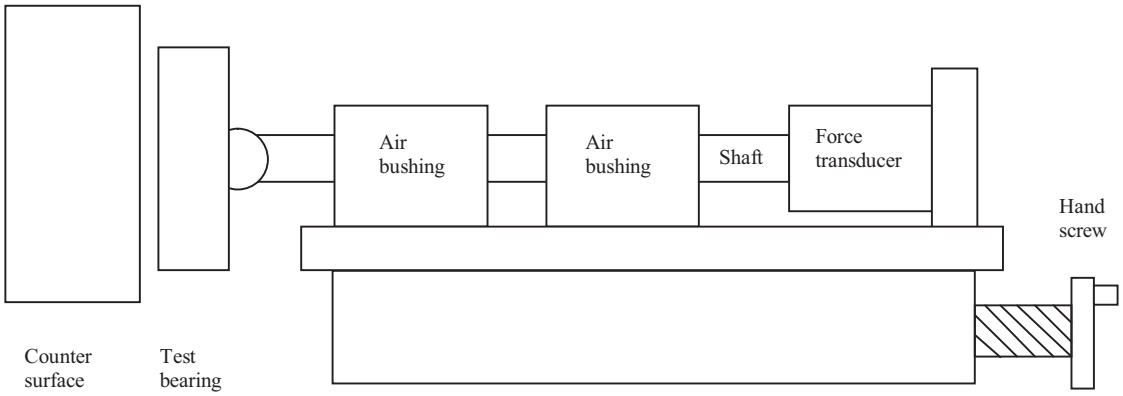


**Figure 2. Schematic of the loading mechanism.**

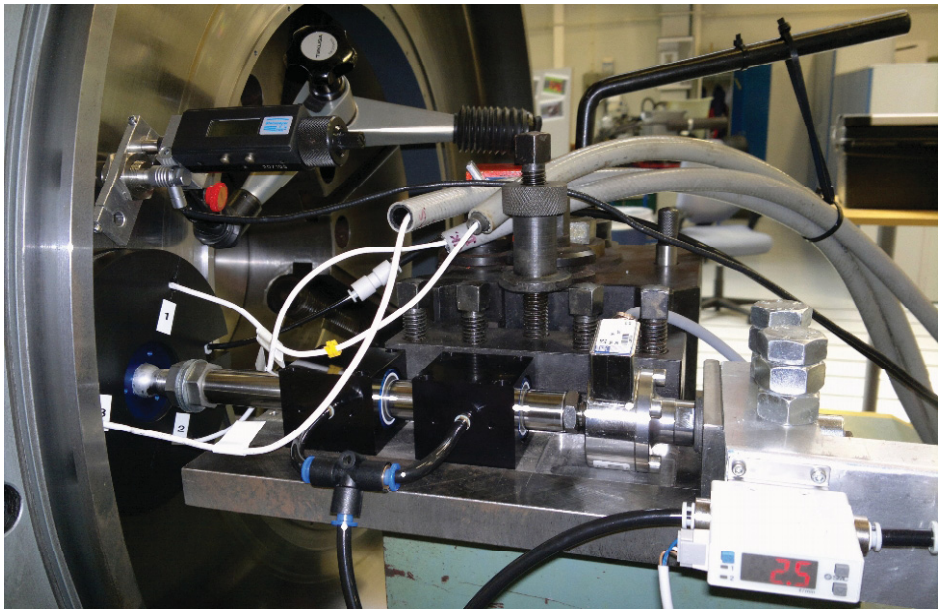

**Figure 3. Close-up photo of the loading mechanism.**

The friction between the force sensor and the end support prevents the rotational movement of the shaft. During the dynamic tests when the test surface is rotating, a series of cup springs can be mounted between the force sensor and the fixed end to allow movement of the shaft caused by axial run out of the counter face. Because force and displacement between bearing and counter surface are measured directly, the flexibility of the structure does not influence the load and gap height measurements, Figures 2 and 3.

### 2.3. Air gap height measurement

Gap height and bearing alignment are measured using three displacement transducers, Figure 4. The transducers are attached to a collar which is directly attached to the bearing. Similar arrangements have been used in axial piston pump research in measuring the lubricant film thickness between the slipper bearing and the swash plate [7], [8]. Eddy current sensors (MicroEpsilon, 1 mm measurement range) were chosen because of their capability to measure displacement in high precision. However, they are sensitive to the material type, surface quality and geometry of the target and inhomogeneities in the material. In order to take this into account, the sensors were each calibrated against the counter surface in their actual usage positions. Zero adjustment of the sensors was done by loading the bearing without air infeed against the counter surface with constant load of 100 N.

### 2.4. Air supply

Aerostatic bearings set high requirements on the quality of the air supply.

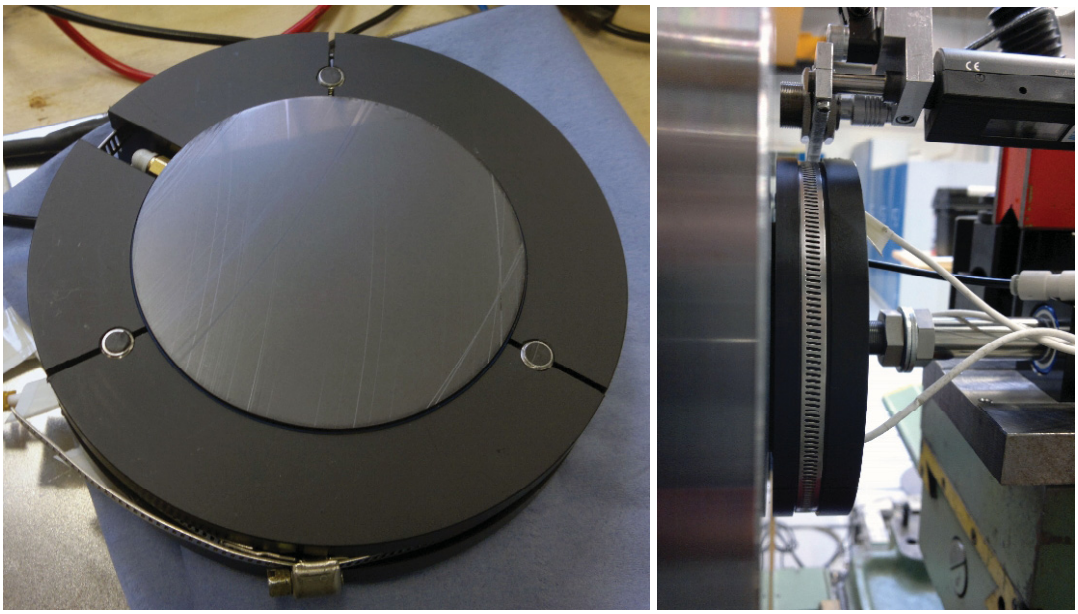

**Figure 4. The air gap height is measured directly using three eddy current sensors attached symmetrically to the bearing.**

The supply pressure is controlled by a precision pressure regulator fitted with a gauge (SMC IR1020). In the tests, the bearing supply pressure was 5.2 bar. Two air flow meters (SMC PFM710, measuring range 0.2 … 10 l/min and FESTO SFE3, measuring range 5 … 50 l/min) were connected to the supply line to measure the air consumption. A service unit consisting of several filters (SMC air filter AF20, mist separator AFM20, micro mist separator AFD20), a pressure regulator (SMC AR20) and a gauge was placed between the pressure source and the system.

### 2.5. Data acquisition

The measurements are recorded on a PC. The data are acquired using a 14-bit analogue-to-digital board located in a personal computer with a sampling rate of 10 kHz. An analogue 2.5 kHz low pass filter is used before sampling to avoid aliasing. The duration of one measurement is typically 10 seconds. After each measurement the data are saved to a file. The analysis of the static measurements is based on the averaged values of each channel. The dynamic measurements are triggered using a laser-type photoelectric sensor (Omron E3C-LD11) with reflective tape glued on the rotating four-jaw chuck. The analysis of the measured data is based on the synchronized averaging of the load, displacement and air consumption.

### 2.6. Test bearings

Two types of flat pad air bearings were used in the study – an orifice type bearing (Nelson Air Corp., FP-C-040) and a porous type bearing (New Way air bearings, S1010001), Figure 5. The diameter of the bearing surface of both bearings was 100 mm. The orifice type bearing has 12 equally spaced orifices on a circumference of diameter 63 mm. The bearings were connected to the shaft by a 20 mm diameter, round end, ball mounting screw.

In the tests, three bearings were used – two porous type bearings (P1, P2) and one orifice type bearing (O1). There were two porous bearings, because after initial tests with the first porous bearing (P1) running against the roll end counter surface some deep scratches were seen on the porous bearing surface, Figure 4. These damages did not seem to have any direct adverse effect on the performance of the bearing and therefore the bearing was still used in the tests against the rotating counter surface. For the tests with a stationary counter surface, however, a new porous bearing (P2) was used. The same orifice compensated bearing (O1) was used in tests both against stationary and rotating counter surfaces.

### 2.7. Counter surfaces

In order to have maximum relative transversal velocity between the bearing and the counter surface, the diameter of the test disk should be maximized. First test disk was a used roll end, 1000 mm in diameter (Figure 6). It had been used for hydrostatic bearing tests so the basic surface quality had been quite good. However, now there were grooves, indentations and bearing metal traces present.

**Figure 5. Test bearings, orifice type (left) and porous type (right)**

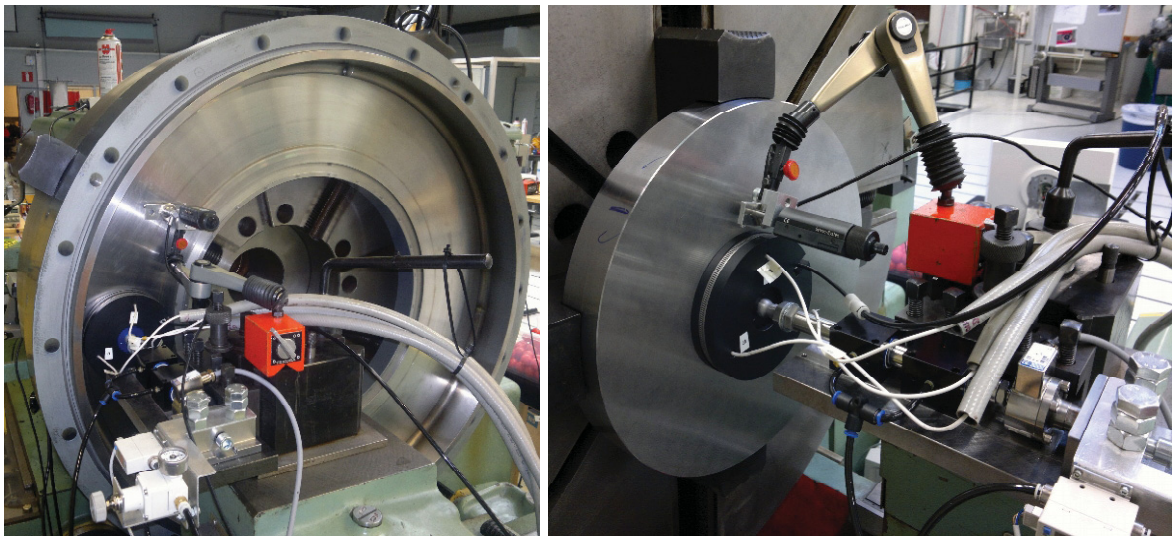

**Figure 6. Test setup for both test surfaces, roll end (left) and test disk (right).**

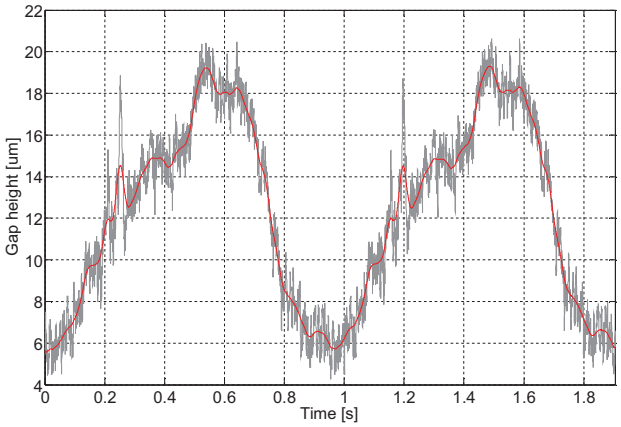


**Figure 7. Gap height vs. time measured with the roll end counter surface. The grey trace is the mean value of the displacement signals of the sensors and the continuous trace is a zero-phase running average. The sine-type shape of the signal is due to the axial run-out of the rotating counter surface.**

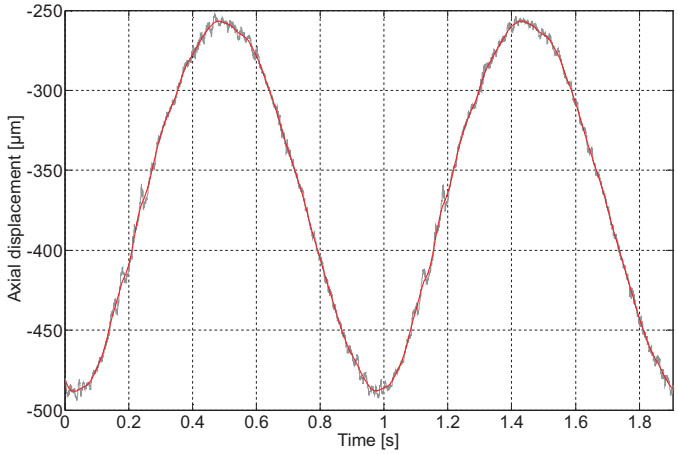


**Figure 8. Axial run-out of counter surface vs. time. The grey trace is the displacement signal and the continuous trace is a zero-phase running average.**

There were also geometrical deviations in the surface which appeared as variations in the run-out at different diameters. The combined effect of these imperfections can be seen in the noisy-looking mean displacement vs. time curve, Figure 7. These imperfections and the variations in the surface quality are seen as sensor noise. Due to its large size and weight the geometrical properties of the surface could not be measured. The surface roughness (Ra) was 0.54 µm in the radial direction and 0.29 µm in the circumferential direction. The axial run-out of the roll end counter surface (approximately 0.25 mm) is shown in Figure 8.

Cup springs were used between the bearing shaft and its attachment to accommodate the motion caused by the axial run-out. The second test disk, 400 mm in diameter, manufactured for test purposes only, was finished by surface grinding. The surface roughness (Ra) was 0.89 µm in the radial direction and 0.76 µm in the circumferential direction. Similar tests were done with both surfaces to see if the surface quality has some effect on the properties and behavior of the bearing. Both counter surfaces were made of steel.

### 2.8. Tests categories

There were two categories of tests:

T1) Tests with a stationary counter surface
- a) Load vs. gap height tests (to determine bearing stiffness and air consumption)
- b) Step tests to determine the response in load and gap height to a compression step change. In these tests, the cup springs were removed.

T2) Tests with a rotating counter surface with axial run-out
- a) Roll end counter surface; speed of rotation 11 rpm, 32 rpm and 63 rpm, radius of rotation $r$ = 0.4 m. In these tests, the cup springs were present.

In tests T1a during the measurement, the load was increased or decreased in steps of 100…200 N. After the adjustment of the load, the bearing was let to stabilize for a period of 60 seconds. In tests T2, The maximum load was set by compressing the springs while the counter-face was at its maximum run-out value.

## 3. RESULTS OF INITIAL MEASUREMENTS

### 3.1. Static measurements

The stiffness of the bearings was measured against both counter surfaces. The load was increased until one of the displacement sensors measuring the air gap indicated contact with the surface. The measurement was done both in the direction of increasing and decreasing values of the load. Measured points and a polynomial fit are depicted in Figures 9 and 10. From this data, the stiffness of the bearing was calculated. For example, against the test disk, the bearings P2 and O1 had maximum stiffness values of 380 N/µm and 104 N/µm at corresponding gap heights of 2 µm and 15 µm (and at 5.2 bar bearing pressure).

During the stiffness measurements, the air consumption in the bearing was measured, Figures 11 and 12.

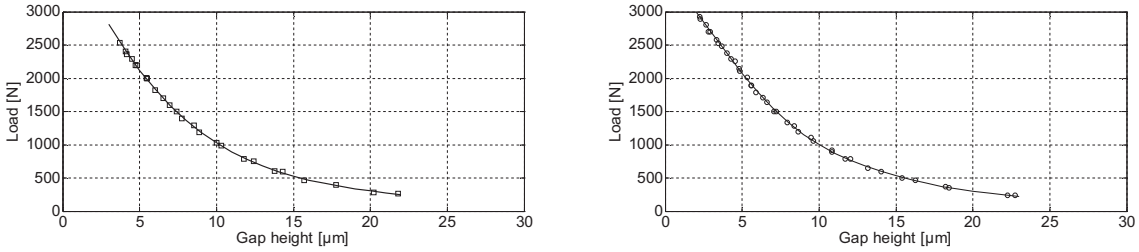


**Figure 9. Load vs. gap height curves of porous type bearing (P2), measured against roll end (left) and test disk (right).**

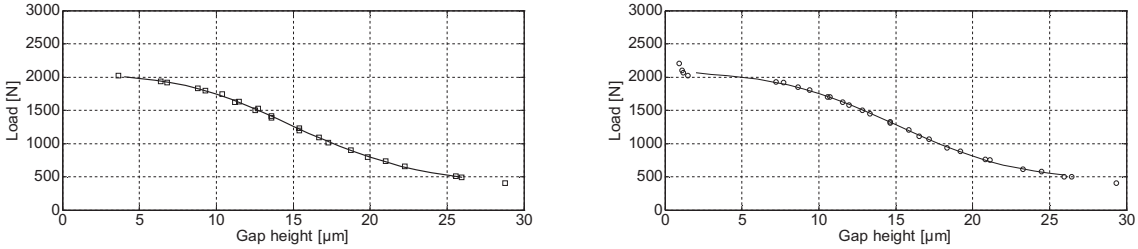


**Figure 10. Load vs. gap height curves of orifice type bearing (O1), measured against roll end (left) and test disk (right).**

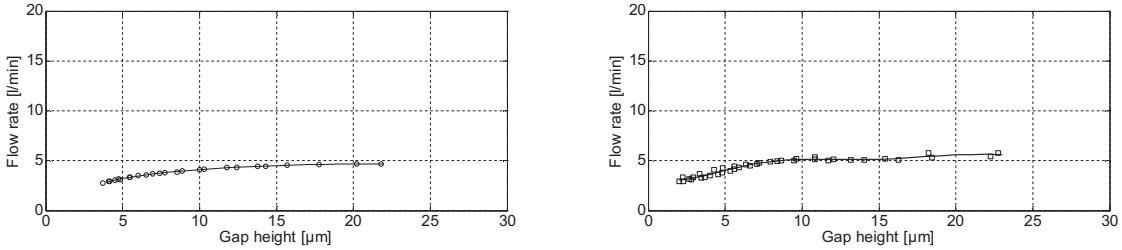


**Figure 11. Air consumption vs. gap height curves of porous type bearing (P2), measured against roll end (left) and test disk (right).**

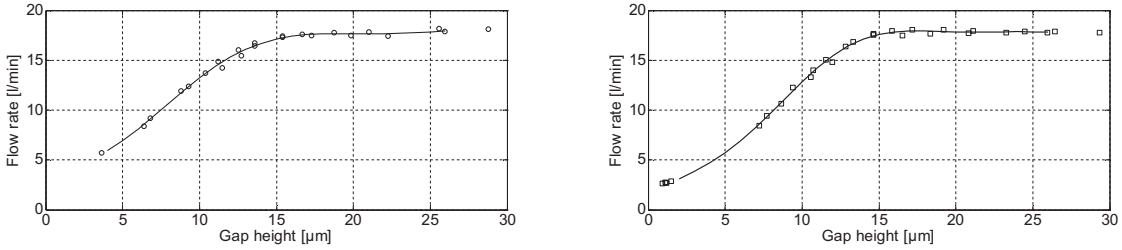


**Figure 12. Air consumption vs. gap height curves of orifice type bearing (O1), measured against roll end (left) and test disk (right).**

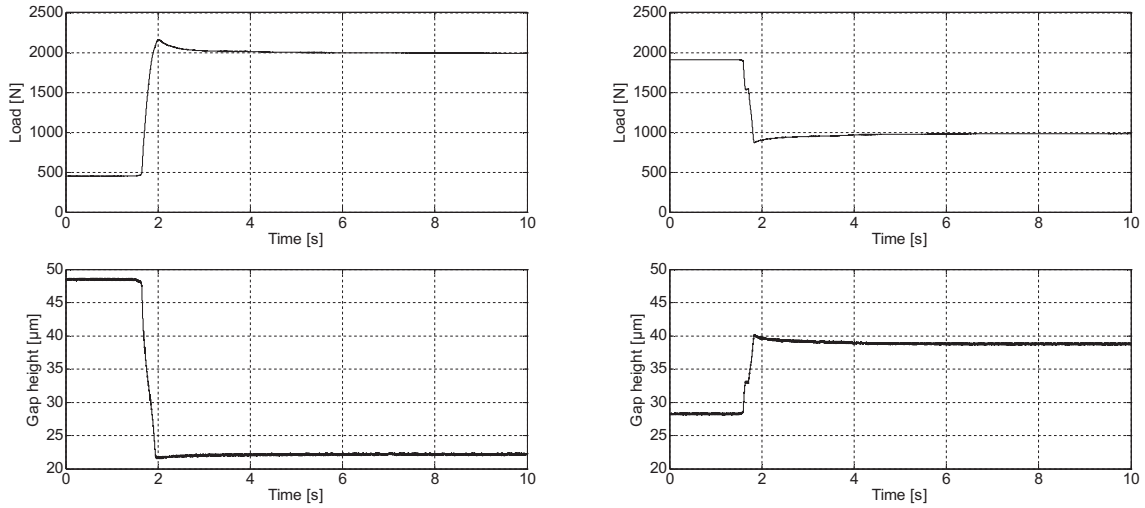


**Figure 13. Step responses (load and gap height) of orifice type bearing, rising (left) and lowering (right) load.**

### 3.2. Step response

During the measurements it was detected that it took some time for the value of the force to stabilize after a change of the compression of the bearing. This was studied by giving the bearing larger stepwise load changes both in the rising and falling directions. The response figures for the orifice type bearing O1 are shown in Figure 13. The response of the porous type bearing was equivalent.

### 3.3. Measurements with rotating counter surface

As an example of results obtained with the T2 category tests, Figure 14 shows the synchronized averaging of the measured bearing load, mean gap height and air consumption. The measurement period for averaging was 60 s and the rotation speed of the roll end was 63 rpm. The results obtained for the lower rotation speeds (11 rpm, 32 rpm) were similar.

Figure 14 also shows the corresponding load vs. gap height graphs. For bearing O1, the load vs. gap height curve measured with a non-rotating counter surface is shown for reference (dashed line, Figure 14d).

Because the two bearings have different load bearing capacities, the maximum load was set close to 2.3 kN for bearing P1 and to approximately 1.9 kN for bearing O1. The load amplitude is determined by the axial run-out of the counter surface and the characteristics of the cup springs.

## 4. DISCUSSION

By adding some simple attachments, such as, air supply, instrumentation and data acquisition it was possible to convert an old, large-size lathe to a test rig for flat pad air bearings. Measurements involving load, air gap height and air consumption are relatively easy to realize in the test rig for bearings pressed against either a stationary or a rotating counter surface. In the four-jaw chuck of the lathe it is also relatively easy to change the counter surface and to adjust its axial run-out. This makes it possible to switch between ideal flat counter surfaces and surfaces featuring run-out, scratches and other imperfections that are likely to be found in industrial machinery.

The possible problems due to the flexibility of the structure of the test rig was taken into account by attaching the displacement transducers to a collar directly attached to the bearing and thus avoiding measurement relying on any moving reference. In addition, the force produced by the pressure distribution in the gap between the bearing surface and the counter surface was measured directly utilizing frictionless air bearing bushings for supporting the load shaft connecting the bearing and the transducer. This way, corrupting friction forces present in ordinary bushings were avoided. Moreover, a more simple load shaft construction was obtained compared to using some kind of flexure joints for connecting the force transducer and the bearing.

The static measurements show that there is a clear difference between the behaviors of the two bearing types. Porous bearing operates with smaller air gap and its stiffness rises rapidly as the air gap get smaller. Orifice type bearing allows higher air gap on its nominal operating range. There is also difference in the air consumption between these bearing types. The larger air consumption in the orifice type bearing corresponds with the larger air gap. The surface quality did not seem to have significant effect on the behavior. The load versus air gap measurements gave practically congruent figures for both test surfaces. These results agree well with the common knowledge about the bearings.

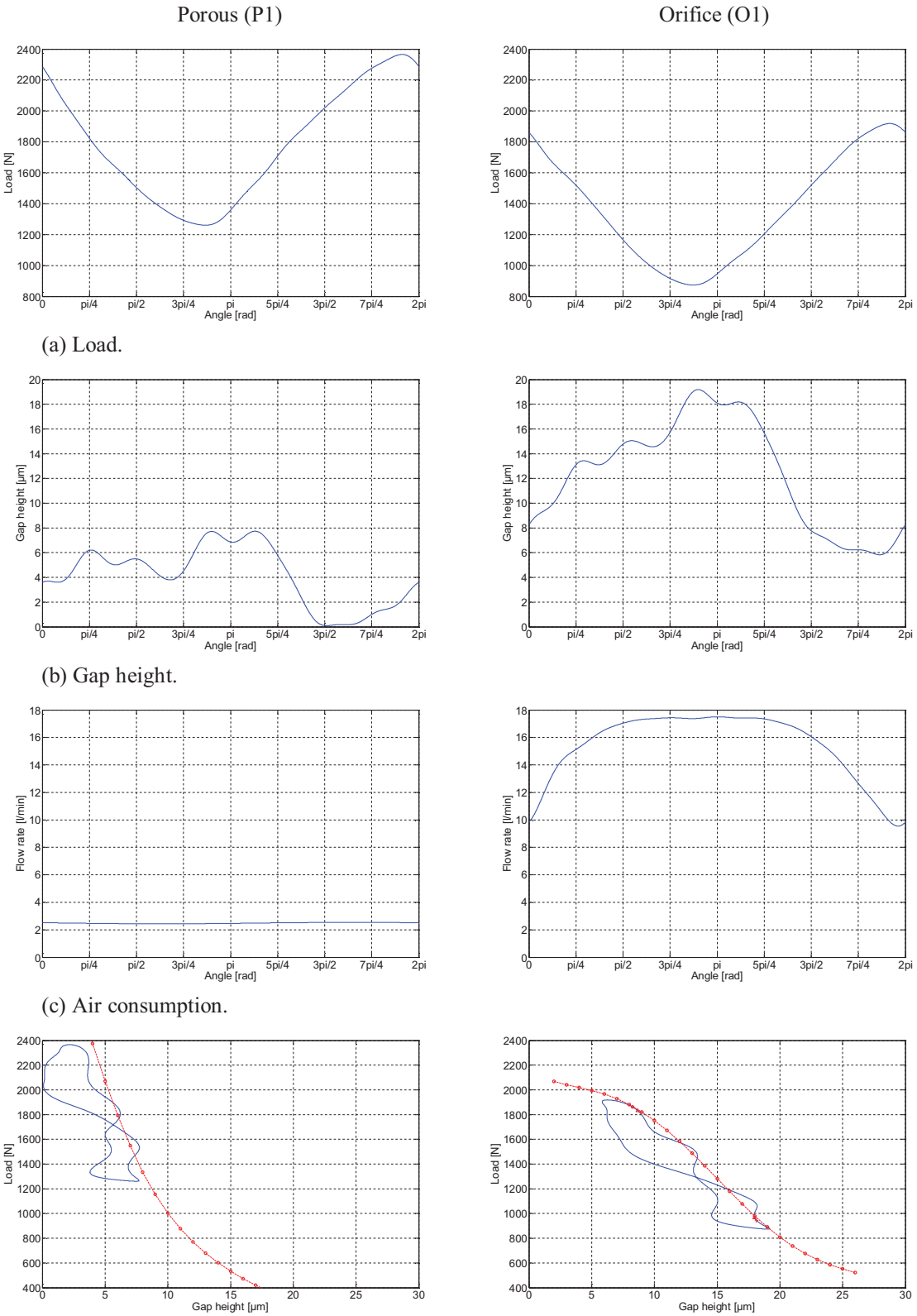


(a) Load.

(b) Gap height.

(c) Air consumption.

(d) Load vs. gap height. Curves with markers are for bearings P2 and O1 against non-rotating surface.

**Figure 14. Cyclic characteristics of porous and orifice compensated bearings obtained by synchronized averaging of 60 rotations. Speed of rotation of the roll counter-face was 63 rpm.**

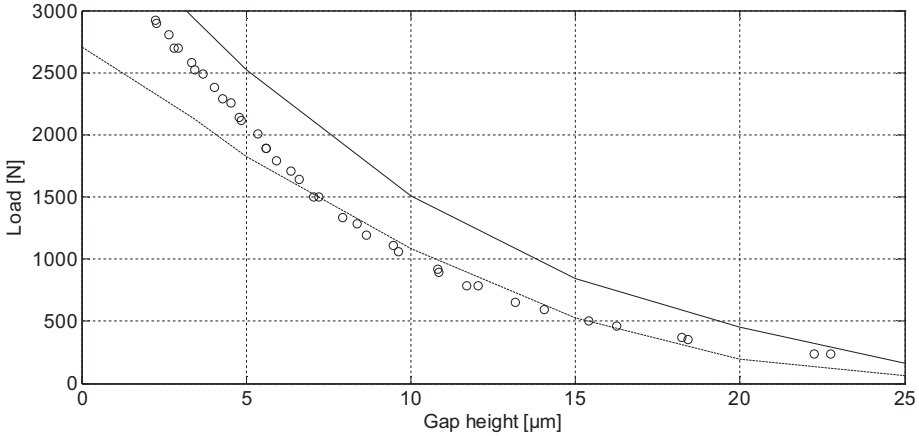


**Figure 15. Lift-load curves [10] for porous bearing with an air supply pressure of 4.1 bar (lower) or 5.5 bar (upper) and measured values (o) with an air supply pressure of 5.2 bar.**

According to the manufacturer's specifications, the load capacity of orifice type bearing is 1710 N at 12.7 µm air gap when air supply pressure is 5.1 bar [9]. Measurements gave a load of approximately 1500 N at that air gap. For the porous bearing the results can be compared with a load-lift curve provided by the manufacturer [10] (Figure 15). Test results agree quite well with specifications giving a little smaller value for load in the region of 7…15 µm air gap.

In the measurements against the rotating counter-face (Figure 14), the basic shape of the gap height curve should be a sine curve, due to the axial run-out of the rotating counter surface. The curve, however, gets modified due to the surface imperfections which superimpose a signal of smaller amplitude and higher frequency on the run-out displacement signal.

In Figure 14 it can be seen that bearing P1 operated at a higher load level and with a smaller air gap height and consequently with smaller air consumption. It can also be seen that the load curve lags somewhat behind the air gap height curve (the phenomenon is more pronounced for bearing P1 than for O1).

For bearing P1, the peak load (2.3 kN) appears to be close to the maximum load value, as the minimum gap height is close to zero. For bearing O1, on the other hand, it appears to be possible to increase the load as the minimum gap height was 6 µm – by increasing the compression the air consumption would also decrease.

Figure 14d highlights the fact that bearing P1 operated at higher loads and with a very narrow air gap, while for bearing O1 the load level was lower and the air gap higher. The difference in the operating characteristics of the bearings is not only a consequence of the bearing structure (porous vs. orifice) alone, but rather a consequence of the combined effect of the bearing structure and the load level.

In comparing the static load-gap height curve to the dynamic curve (Figure 14d), it can be seen that for a given gap height the bearing force was generally lower when the bearing was running against the rotating counter surface with axial run-out and surface imperfections than when the bearing was compressed against the non-rotating counter surface of good surface quality.

While the development work is still ongoing, the overall impression after the initial tests reported here is that the test rig is a promising platform for studies involving either large-size counter surfaces, or the need to change counter surfaces (due to, e.g., different surface treatments or coatings), or the development of new large-size air bearing solutions for industrial purposes. Of course, the test rig can also play its part in validating computational bearing models.

A target for further development would be an actuator for producing precise and dynamic loading. The current load production – hand screw – is adequate for static measurements. For example, varying loads used in frequency response studies call for a relatively fast actuator with good controllability. To some extent, the current displacement transducers are a limiting factor. The eddy current transducers now in use require that the counter surface be of ferromagnetic material. However, usually the counter surface material for air bearings is non-corroding (and therefore often non-ferromagnetic) because of the corrosion risk associated with condensation of water due to the cooling effect of the air escaping from the bearing gap.

Due to the early stage of this research it is premature to say what the measurement uncertainty of the test environment is. The major sources of error

are related to the structure, measurements, instrumentation and air supply. Regardless of direct measurement of air gap and load, misalignments and elasticity of structure may cause some error. To minimize errors related to instrumentation, sensors and their amplifiers are calibrated carefully when possible. The error in the gap height measurement is in the region of ±1 μm and in the force measurement ±25 N. The pressure and air flow measurements are not calibrated and they are also the most inaccurate quantities of the system.

## 5. REFERENCES


[1] M. Fourka, Y. Tian and M. Bonis, "Prediction of air thrust bearings by numerical, analytical and experimental methods", Wear, 198, pp. 1-6, 1996.

[2] D.A. Boffey, A.A. Barrow and J.K. Dearden, "Experimental investigation into the performance of an aerostatic industrial thrust bearing", Tribology international, Vol 18, No 3, pp. 165-168, 1985

[3] G. Aguirre, F. Al-Bender and H. Van Brussel, "A multiphysics model for optimizing the design of active aerostatic thrust bearings", Precision Engineering 34, pp. 507-515, 2010.

[4] Y.B.P. Kwan and J. Corbett, "A simplified method for the correction of velocity slip and inertia effects in porous aerostatic thrust bearings", Tribology International, Vol. 31, No. 12, pp. 779-786, 1998.

[5] G. Belforte, F. Colombo et al. "Comparison between grooved and plane aerostatic thrust bearings: static performance", Meccanica, Vol. 46, pp. 547-555, 2011.

[6] F. Al-Bender, "On the modeling of the dynamic characteristics of aerostatic bearing films: From stability analysis to active compensation", Precision Engineering 33, pp. 117-126, 2009.

[7] Donders, S.J.M., Kolbenmaschinen für HFA-Flüssigkeiten - Verlustanteile einer Schrägscheiben-einheit, Dissertation, RWTH Aachen, Verlag Mainz, Aachen, 1999.

[8] M. Rokala, O. Calonius, K.T. Koskinen and M. Pietola, "Study of lubrication conditions in slipper-swashplate contact in water hydraulic axial piston pump test rig", 7th JFPS International Symposium on Fluid Power, 15-18 September, Toyama, Japan, 2008.

[9] Nelson Air Corp., FP Series Round Flat Pad Air Bearings, http://www.nelsonair.com/NA_prods_flat-pad_fp.htm, Accessed July 2011.

[10] New Way Air Bearings, New Way 100mm Flat Round Air Bearing Lift-Load Curve, http://www.newwayairbearings.com/Air-Bearings-Flat-Round-100mm, Accessed July 2011.